AMLR Asociația de Medicină de Laborator din România

Romanian Journal of Laboratory Medicine 2026;34(1):27–38

ORIGINAL RESEARCH

DOI:10.2478/rrlm-2026-0001

Mechanistic study of novel arylpiperazine derivative NAF19 in prostate cancer treatment based on network pharmacology approach

Hua Jiang[1*], Mingzhen Xu[1], Songsong Jiang[1], Weiqiang Huang[2], Hong Chen[3]

1. Department of Urology, The Fifth Affiliated Hospital of Zunyi Medical University, China
2. The Department of Biological and Pharmaceutical Sciences, Zhuhai Campus of Zunyi Medical University, China
3. Luoyang Key Laboratory of Organic Functional Molecules, College of Food and Drug, Luoyang Normal University, China

ABSTRACT

Background: Our preliminary studies identified the arylpiperazine derivative NAF19 as a promising therapeutic agent against prostate cancer, though its precise mechanisms remained unclear.

Methods: Network pharmacology was utilized to pinpoint both therapeutic targets and disease-related targets. Functional assessments of cells were conducted using the CCK-8 method and wound-healing assays to analyze the effects of NAF19 on LNCaP cell proliferation and migration, respectively. The effect of NAF19 on the cell cycle progression of prostate cancer cells was examined using flow cytometry, while phosphorylation of AKT and PI3K was assessed using Western blotting.

Results: The anti-proliferative activity of NAF19 increased with higher doses and longer durations of treatment. The wound healing assay confirms its strong inhibitory effect on cell migration. Western blotting results indicate that NAF19 influences EMT-related protein expression, leading to elevated E-cadherin and decreased Vimentin and N-cadherin levels. Further mechanistic investigation showed that NAF19 significantly reduced the expression of CXCR4, as well as phosphorylated PI3K and Akt proteins. Western blot results confirmed that NAF19 downregulated Skp2 while increasing the levels of p27 and p21, suggesting involvement of the Skp2/p27/p21 signaling pathway. Molecular docking analysis demonstrated that NAF19 binds strongly to CXCR4, exhibiting a binding energy of-9.6 kcal/mol.

Conclusions: This investigation confirms that NAF19 acts as a new CXCR4 antagonist, effectively suppressing several cancer-promoting pathways in prostate cancer, such as PI3K/AKT signaling, cell cycle advancement, and EMT.

Keywords: arylpiperazine derivative, CXCR4, network pharmacology, prostate cancer

Received: 21 August 2025; Accepted: 12 November 2025; Published: 21 January 2026.

INTRODUCTION

Prostate cancer (PCa) is among the most common malignancies in the global male genitourinary system, particularly in middle-aged and elderly populations. In 2020, worldwide cancer statistics reported approximately 10.06 million new cases and 5.53 million deaths among males, with PCa accounting for 1.41 million new cases and 380,000 fatalities (mortality-to-incidence ratio: 27%). Notably, China documented 120,000 new PCa cases and 50,000 deaths, yielding a significantly higher mortality-to-incidence ratio of 41.7% [1]. According to the 2025 U.S. cancer report, PCa prevalence dominates male malignancies, constituting about 30% of cases [2].

Naftopidil is classified as an arylpiperazine derivative and exhibits selective antagonism toward both α1A and α1D adrenoceptor subtypes. By lowering dihydrotestosterone concentrations within prostate tissues and cells, this compound facilitates apoptotic processes. Thus, naftopidil is currently utilized in the management of benign prostatic hyperplasia (BPH) [3]. Furthermore, research has shown that NAF significantly suppresses the growth of prostate cancer cells, such as PC-3 and LNCaP, while promoting apoptosis [4-6]. Capitalizing on its modifiable structure, our team synthesized the novel arylpiperazine derivative NAF19 (Figure 1) through side-chain modification of naftopidil. In our group's previous studies, the IC_{50} value of naftopidil was found to be greater than 50 μM in prostate WPMY-1 cells, and 42.10, 22.36, and 34.58 μM in prostate cancer PC-3, LNCaP, and DU145 cells, respectively. In contrast, NAF19 exhibited significantly higher potency, with an IC_{50} > 50 μM in WPMY-1 cells and IC_{50} values of 1.23, 2.32, and 0.87 μM in PC-3, LNCaP, and DU145 cells, respectively [7,8]. However, its precise mechanism of action remains unclear.

* Corresponding author: Hua Jiang, Department of Urology, The Fifth Affiliated Hospital of Zunyi Medical University, China. E-mail: jianghua426@zmu.edu.cn

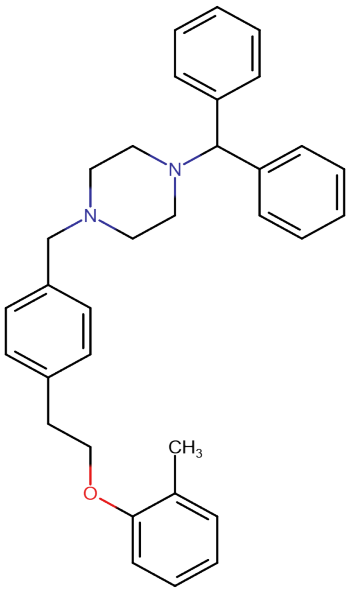

Figure 1. Novel naftopidil derivative (NAF19) structure.

Network pharmacology—an emerging interdisciplinary field integrating network biology, pharmacology, bioinformatics, and systems biology—transcends the traditional "one-target-one-drug" paradigm by constructing biological networks to decipher disease pathogenesis and drug mechanisms [9,10]. Leveraging this approach, we systematically identified NAF19's key targets, molecular pathways, and biological processes in PCa treatment, followed by experimental validation. This study provides a theoretical foundation for developing novel anti-PCa therapeutics.

METHODS

Ethics approval was not required for this study.

Reagents

DMEM medium and 10% fetal bovine serum (FBS; Gibco, USA; Lot No.: 8115130, 42G437k); CCK-8 assay kit (PerkinElmer, China; Lot No.: AR119); dimethyl sulfoxide (DMSO; Suzhou Lianxiong Fine Chemical Technology Co., Ltd.; Lot No.: 16040302); primary antibodies: p-PI3K, PI3K, p-AKT, AKT, CXCR4, E-cadherin, N-cadherin, Vimentin, Skp2, p27, p21(Abcam, UK; Lot No.: ab278545, PI3K p85, ab182651, ab52627, ab108202, 181020, ab287970, ab280375, ab16700, SKP2, 64949, ab109520); secondary antibody: HRP-labeled goat anti-rabbit (Beijing Bioss Biotechnology Co., Ltd.; Lot No.: BIR703).

Cell culture

The LNCaP cell line was acquired from Procell Life Science & Technology Co., Ltd. located in Wuhan. LNCaP cells were grown in DMEM enriched with 10% FBS and 1% penicillin-streptomycin at 37 °C with 5% CO_2. Media were replaced at two to three-day intervals. Subculturing was performed once the confluence exceeded 85%.

CCK-8 assays

LNCaP cells in logarithmic growth were inoculated in 96-well plates. A blank control group was included, and six concentrations (0, 2, 4, 6, 8, and 10 µmol/L) were evaluated. Each concentration was set up in six replicate wells. The supernatant was aspirated from cells incubated for 24 or 48 hours, followed by the addition of 100 µL of fresh medium and 10 µL of CCK-8 solution to each well. The plate was incubated for 0.5 hours. The absorbance at 450 nm was measured using a microplate reader.

Colony formation assays

Cells in good growth condition were seeded in culture dishes at 1×10^3 cells/well, treated with different concentrations of NAF19, and cultured at 37°C with 5% CO_2 for about 14 days, with regular observation of cell growth status and medium color changes during this period. Upon completion of the incubation, cells were fixed using 4% paraformaldehyde (PFA) and subsequently stained with a 0.5% crystal violet. Visible colonies were enumerated under a microscope, and the rate of colony formation was determined by calculating (number of colonies / number of cells seeded) × 100%.

Wound healing assays

Logarithmic growth phase LNCaP cells were plated in 6-well plates. Upon reaching 95–98% confluence, 20 mg/L of mitomycin C was introduced into each well and incubated for 2 hours to suppress cell proliferation. A scratch wound was generated in the monolayer using a sterile 10 µL pipette tip. After rinsing gently with D-PBS, cells were treated with serum-free medium supplemented with varying concentrations of NAF19 (0 and 8 µmol/L). Each treatment was performed in triplicate. Images were captured at 0 and 24 hours post-treatment. For each time point, six randomly chosen fields were analyzed, and the extent of wound closure was quantified with ImageJ software.

EdU assays

Transfected cells were inoculated in 96-well plates and exposed to EdU-supplemented medium for 2 h at 37°C and 5% CO_2. After this incubation, the cells were fixed (4% PFA, 20 min) and then labeled with Apollo dye for an additional 30 minutes. Finally, nuclei were counterstained with DAPI for 30 minutes at ambient temperature prior to image acquisition. The experiment was performed in triplicate.

Construction of molecular networks

Acquisition of potential targets for NAF19

The SMILES string and two-dimensional molecular structure of NAF19 were obtained from PubChem. The SMILES of NAF19 is CC1=CC=CC=C1OCCC1=CC=C(CN2CCN(CC2)C(C2=CC=CC=C2)C2=CC=CC=C2)C=C1. The structural formula of NAF19 is shown in Figure 1. Potential

pharmacological targets were predicted using SuperPred, PharmMapper, and SwissTargetPrediction. Target protein and gene information was standardized using the UniProt database.

Identification of PCa-related target genes

The keyword "Prostate cancer" was used to mine potential disease targets from the OMIM, DrugBank, GeneCards, and CTD databases. Targets with a GeneCards relevance score ≥10 or equivalent confidence in CTD were selected. Duplicate entries were removed, and the remaining targets were consolidated.

Construction of PPI networks for shared targets between NAF19 and PCa

The drug-target regulatory network was visualized using Cytoscape (v3.10.3). Overlapping genes between drug and disease targets were identified, and their protein-protein interaction (PPI) networks were developed using STRING (v11.0) with a minimum confidence score of 0.4. The resulting PPI network was further analyzed in Cytoscape, with node importance ranked by Degree centrality.

Functional enrichment analysis and network integration

Functional enrichment analyses of overlapping targets were conducted using clusterProfiler (v4.10.0) in R. GO categories, including biological process (BP), cellular component (CC), and molecular function (MF), along with KEGG pathways, were examined. Terms with $p < 0.05$ and counts >1 were considered significant. An integrated "drug-target-disease-pathway" network was constructed to visualize multi-level interactions.

Molecular docking verification

The top 6 hub targets from PPI analysis were docked with NAF19 using AutoDock Vina. Ligand 3D structures were generated from SMILES via Open Babel (https://openbabel.org/), while protein structures were retrieved from the Protein Data Bank. Preprocessing (dehydration, hydrogenation, charge assignment) was performed using AutoDockTools and PyMOL. Binding affinity was evaluated with docking energy thresholds of <-5 kJ/mol, indicating strong interactions.

Cell cycle analysis

LNCaP cells were grown with 8 µmol/L NAF19 for 48 h, harvested, and fixed. After staining with Solution A/B/C (10 min each), cell cycle distribution was analyzed using a BD Aria III flow cytometer. Data processing was performed with ModFit LT software, with untreated cells as negative controls.

Western blot (WB)

LNCaP cells were grown with NAF19 (4/8 µmol/L) for 48 h. Proteins were isolated with RIPA lysis buffer, quantified with the BCA assay, and adjusted to a concentration of 2 g/L. Following electrophoresis and transfer, the blots were treated overnight at 4 °C with primary antibodies. They were then exposed to HRP-linked secondary antibodies. Band intensities were quantified using ImageJ (n=3).

Statistical analysis

All statistical evaluations were performed with SPSS version 22.0, and results are expressed as mean ± standard deviation. GraphPad Prism 8 was used for plotting. Differences between the two normally distributed groups were compared using the independent samples t-test. Multiple groups were compared using one-way analysis of variance (ANOVA) and LSD post-hoc tests. All analyses were two-sided, and $p < 0.05$ was considered statistically significant.

RESULTS

NAF19 inhibits LNCaP cell proliferation

The IC_{50} of NAF19 against LNCaP cells was determined through CCK-8 assays to evaluate its anti-proliferative activity. Results demonstrated dose- and time-dependent growth inhibition, with IC_{50} values of 8.004 µmol/L (24 h) and 5.204 µmol/L (48 h) (Figure 2A). Colony formation assays confirmed significant suppression of clonogenic capacity (Figure 2B), while EdU incorporation assays revealed markedly reduced DNA synthesis in treated groups (8 µmol/L, 48 h; $p < 0.01$ vs controls, Figure 2C).

NAF19 suppresses LNCaP cell migration

Wound healing assays evaluated NAF19's impact on cellular motility. Treatment with 8 µmol/L NAF19 for 24 h significantly impaired migration capacity compared to untreated controls (Figure 3A), corroborating its anti-metastatic potential.

NAF19 modulates genes related to cell migration

To investigate the molecular mechanisms affecting cell migration and invasion, the influence of NAF19 on EMT-related genes and proteins involved in migration was assessed using wound healing assays and Western blot analysis.

E-cadherin, a critical epithelial marker, showed a significant upregulation in protein expression following NAF19 treatment compared to the control group. Conversely, N-cadherin, a mesenchymal marker, exhibited a marked reduction in protein expression after NAF19 treatment. Additionally, Vimentin, another mesenchymal marker, was downregulated in its protein expression upon NAF19 treatment(Figure 3B). These results confirm that NAF19 regulates the expression of EMT-related proteins, thereby influencing cell migration and invasiveness. By modulating these key markers, NAF19 appears to play a role in reversing EMT, potentially contributing to its anti-metastatic effects.

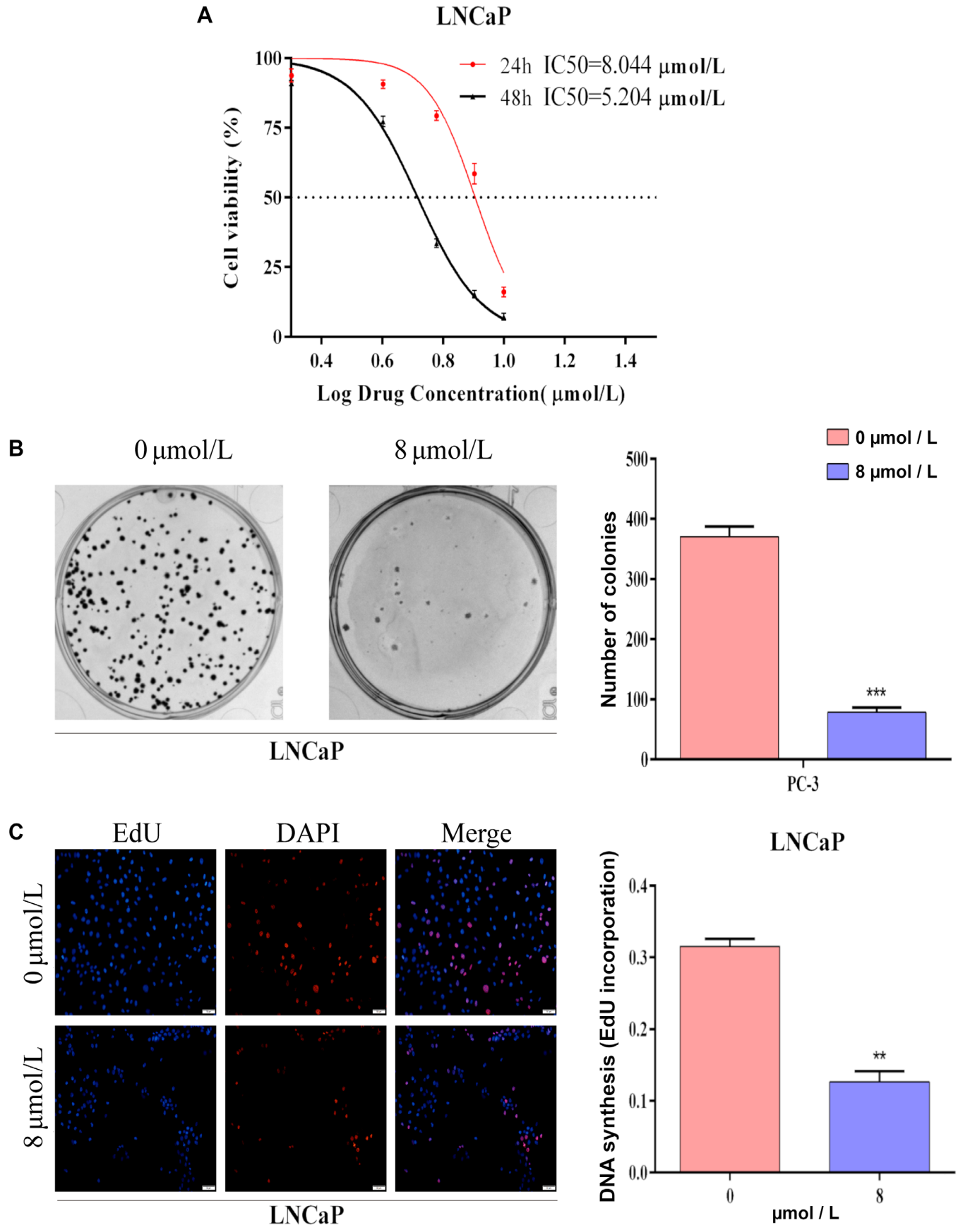

Figure 2. Effects of NAF19 on the proliferation of prostate cancer LNCaP cells

(A) Inhibitory effects of NAF19 at varying concentrations on LNCaP cell viability, as determined by CCK-8 assay; (B) Impact of 8 μmol/L NAF19 treatment on the clonogenic capacity of LNCaP cells; (C) EdU incorporation assay illustrating the suppressive role of NAF19 in LNCaP cell proliferation.

Development and validation of a PPI network for the identification of critical targets

The regulatory relationship between drugs and target genes was visualized through network diagrams (Figure 4A). By intersecting drug target genes with disease target genes, we identified a set of intersection genes (Figure 4B), totaling 21 genes. Utilizing the STRING database, an interaction network among proteins was established using the overlapping genes, incorporating 18 genes within this network. A criticality analysis was performed on each node within the interaction network, where redder colors indicate nodes with more connections, signifying greater importance (Figure 4C).

Functional enrichment analysis on common genes: Insights into GO terms and KEGG pathways

An enrichment analysis focusing on GO functions and KEGG pathways was conducted for the 18 intersection genes from the interaction network. The GO enrichment yielded 492 significantly enriched terms (Figure 5A). Among these, the most significant BP term was regulation of heart rate, CC was T-tubule, and MF was ammonium ion binding. For KEGG pathway enrichment, 14 significant pathways were identified, with the most notable being Pathways in cancer and PI3K-Akt axis (Figure 5B). Additionally, a network diagram illustrating the relationships between enriched pathways and genes was created (Figure 5C).

NAF19 inhibits phosphorylation of PI3K/Akt pathway-related proteins in LNCaP cells

Based on the preceding cellular phenotype experiments, NAF19 demonstrates an inhibitory effect on PCa cell proliferation. To further elucidate the mechanism by which NAF19 exerts its therapeutic effects on prostate cancer, we treated LNCaP cells with 8 µmol/L NAF19 for 48 hours. A group containing 0.3% DMSO served as the blank control (Figure 6). The results indicate that NAF19 significantly reduces the levels of CXCR4 and phosphorylated proteins p-Akt and p-PI3K in LNCaP cells relative to the controlscompared to the controls. These findings suggest that NAF19 inhibits the activity of the PI3K-Akt axis in LNCaP cells.

NAF19 influence on cell cycle in LNCaP cells

To verify the network pharmacology-based predictions on the potential role of NAF19 in inhibiting prostate cancer cell proliferation via cell cycle modulation, flow cytometric analysis was utilized to assess its effects on LNCaP cells (Figure 7A). The results demonstrated that exposure to 8 µmol/L NAF19 resulted in a markedly higher percentage of cells in the G1 phase ($p < 0.01$), along with a marked decrease in S phase cells relative to the controls ($p < 0.05$). These findings suggest that NAF19 might suppress the LNCaP cells' proliferation by inducing cell cycle arrest at the G1 stage.

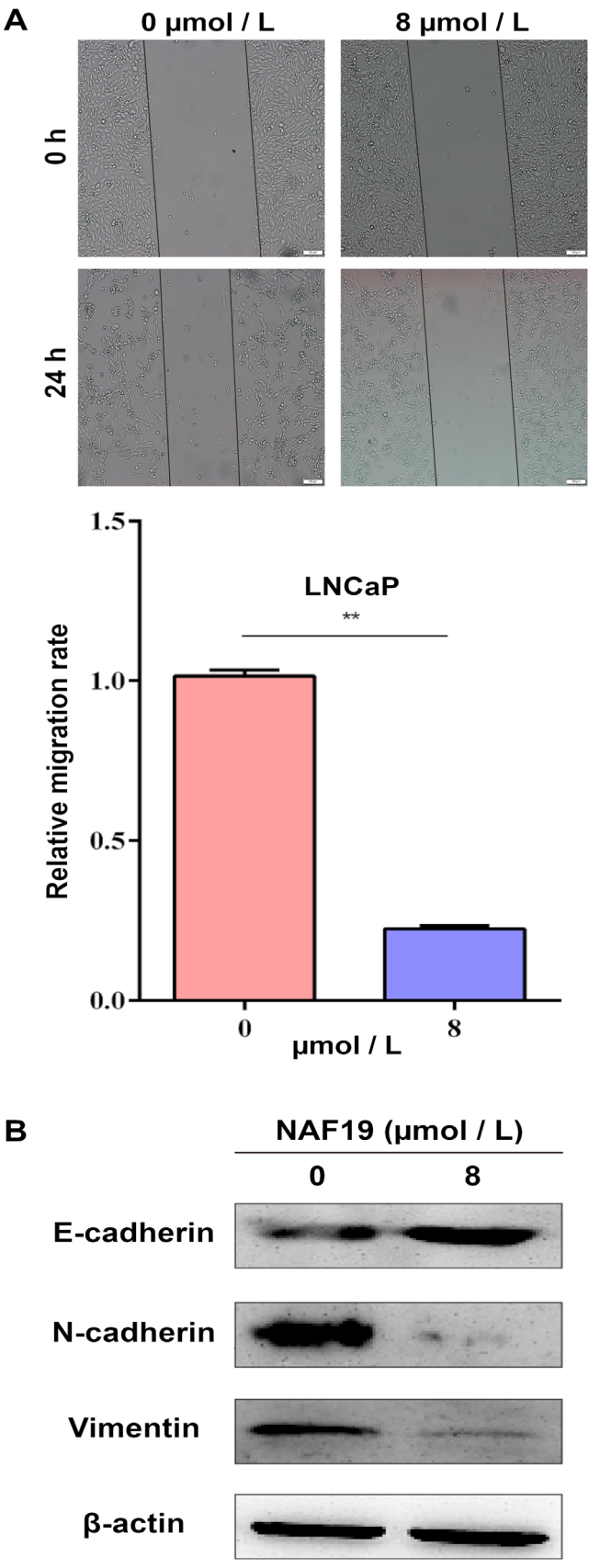

Figure 3. Effect of NAF19 on LNCaP cells migration

(A) Wound healing assay demonstrating the inhibitory effect of NAF19 on LNCaP cell migration; (B) Western blot analysis of NAF19-regulated expression of cell migration-related genes.

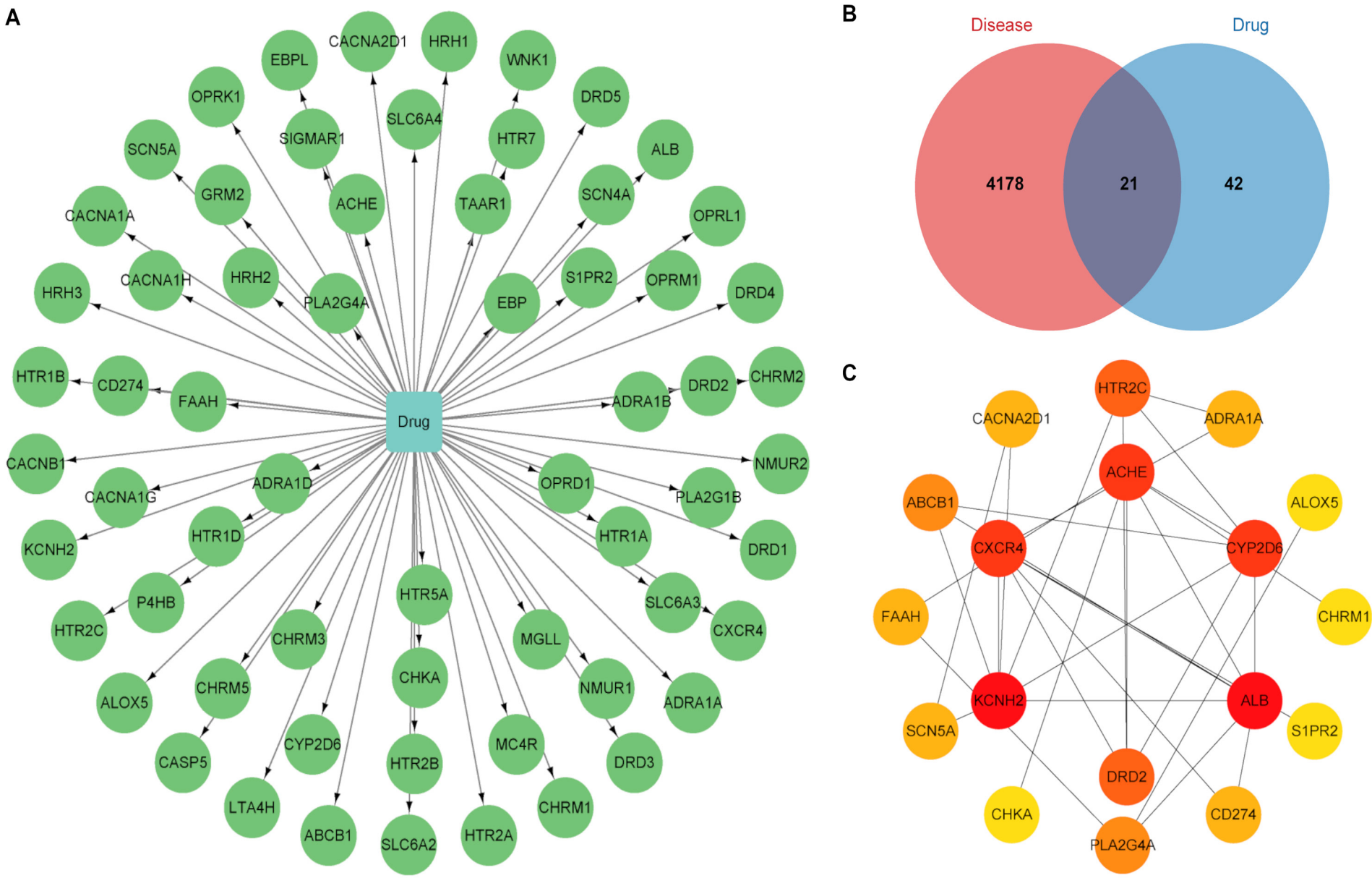

Figure 4. Construction of protein-protein interaction (PPI) network and identification of key targets based on network pharmacology

(A) Drug-target interaction network illustrating the regulatory relationships; (B) Venn diagram depicting the overlapping targets between drug-related and disease-related genes; (C) Protein-protein interaction network of the shared targets.

Role of NAF19 in modulating cell cycle-associated protein levels in PCa cells

Research has found that CXCR4 can affect the expression of Skp2 and its downstream related genes through the regulation of the signaling protein PI3K/Akt [11]. To gain deeper insight into the mechanistic basis of NAF19-mediated cell cycle regulation in PCa cells, WB was employed to quantify the levels of key cell cycle-associated proteins, namely, Skp2, p27, and p21, as predicted through network pharmacology. Among these, p27 and p21 are known downstream regulators of Skp2.

Following a 48-hour treatment of prostate cancer cells with 8 µmol/L NAF19, Skp2 protein levels showed a notable reduction, while p27 and p21 expression were significantly upregulated relative to the control (Figure 7B). These findings suggest that NAF19 may inhibit PCa cell proliferation by modulating the Skp2/p27/p21 signaling pathway, thereby influencing cell cycle progression.

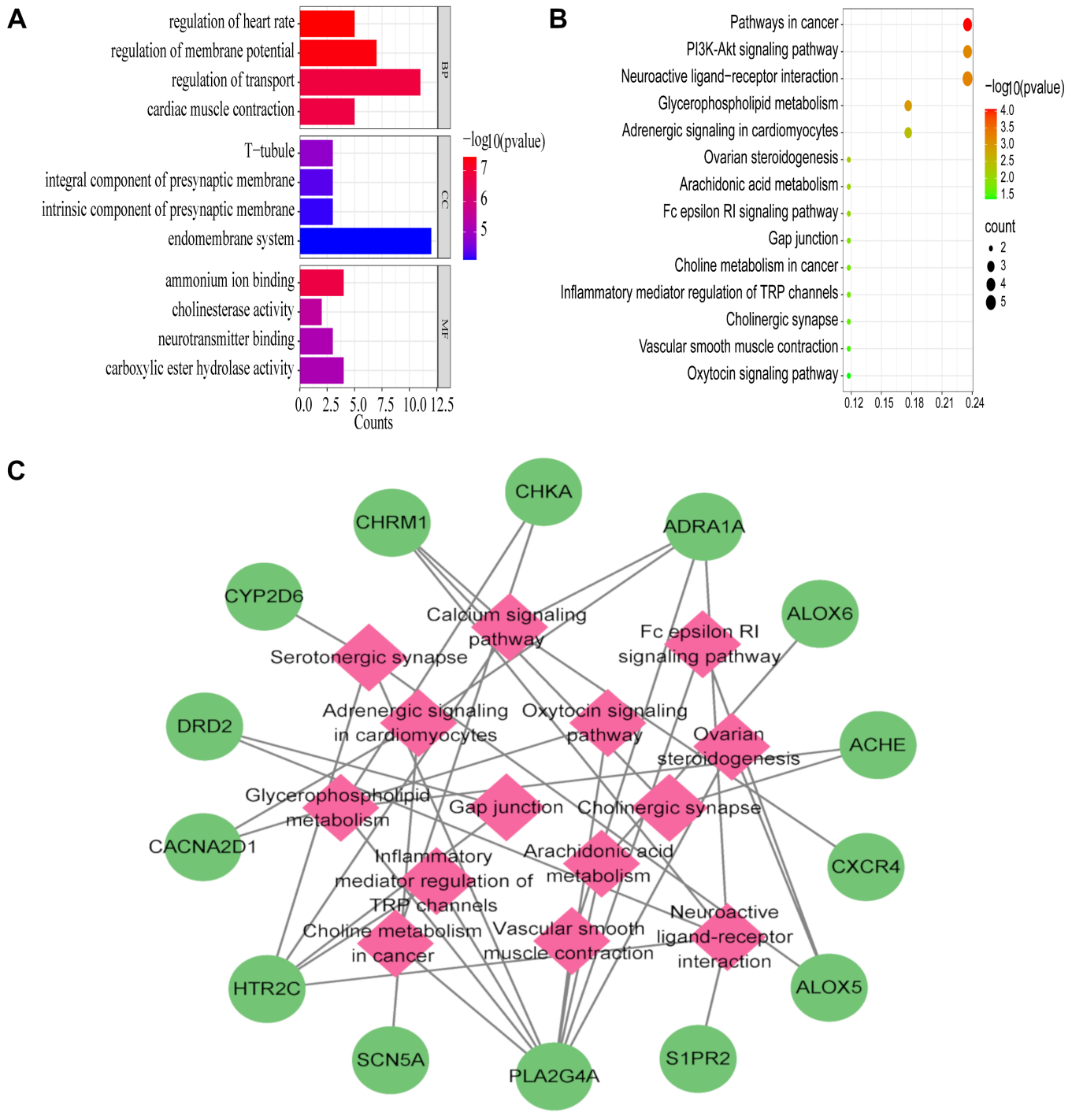

Figure 5. Functional enrichment of overlapping genes in GO and KEGG

(A) GO enrichment of 18 hub overlapping genes; (B) KEGG pathway enrichment of the 18 hub overlapping genes; (C) KEGG pathway-gene network illustrating functional associations between enriched pathways and core genes.

Molecular docking study

To further investigate whether NAF19 regulates the expression of downstream proteins Skp2, p27, and p21 through direct binding with CXCR4, we performed molecular docking between NAF19 and the key target protein CXCR4 (Figure 7C). In the provided diagrams, hydrogen bonds are depicted as solid blue lines, hydrophobic interactions as black dashed lines, salt bridges as yello dashed lines, and π-π interactions as green dashed lines. The calculated binding energy was-9.6 kcal/mol, indicating a strong affinity between NAF19 and CXCR4. These findings imply that NAF19 could bind directly to CXCR4, thereby possibly modulating the levels of key downstream regulators of the cell cycle, including Skp2, p27, and p21.

DISCUSSION

PCa is a common malignancy in elderly males. With its increasing incidence, PCa has become a major disease that significantly impacts male life expectancy and quality of life. While research indicates a favorable five-year survival outlook for localized prostate cancer, the majority of patients remain asymptomatic during initial disease progression. As a result, the disease is often diagnosed at an advanced stage, where it tends to develop resistance to treatment and progress into lethal castration-resistant prostate cancer (CRPC), presenting a major challenge in clinical management [12]. Therefore, improving therapeutic efficacy, prolonging patient survival, and reducing mortality remain urgent clinical priorities.

Our previous research identified NAF19, a novel arylpiperazine compound with anti-resistance properties, as having strong inhibitory effects on prostate cancer cells [7]. However, its underlying mechanisms were not fully understood. Here, network pharmacology was employed to evaluate potential therapeutic targets, key signaling pathways, and relevant biological processes associated with the anti-prostate cancer effects of NAF19.

PCa is an androgen-related malignancy [13]. The progression and metastasis of tumors are significantly influenced by the functionality of the androgen receptor (AR) [14]. Activation of AR-regulated genes by androgens facilitates the proliferation, differentiation, and metastatic spread of PCa cells [15]. Therefore, targeting AR remains one of the primary strategies in PCa therapy [16,17]. However, long-term androgen deprivation therapy can aberrantly activate the PI3K/Akt pathway [18], thereby enhancing tumor cell survival by suppressing apoptosis.

Emerging studies suggest that the PI3K/Akt axis is closely linked to PCa progression [19-23]. Hence, this pathway represents a promising non-AR-targeted therapeutic strategy. Based on KEGG enrichment analysis derived from our network pharmacology data, the PI3K/Akt signaling pathway exhibited the greatest number of

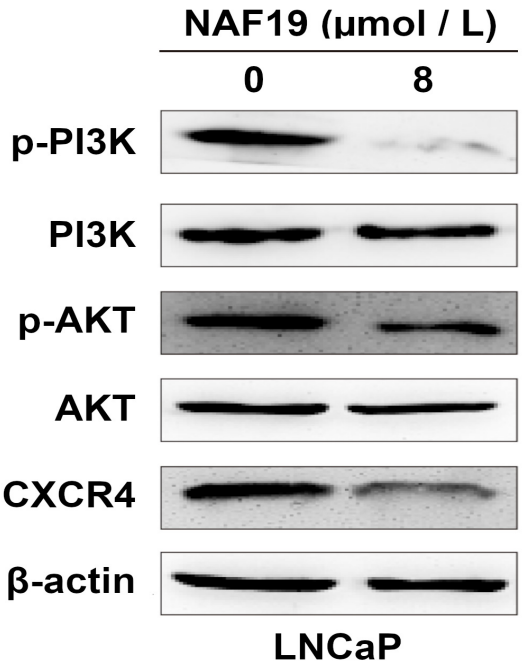

Figure 6. Western blots showing NAF19-altered levels of CXCR4 and its key downstream target proteins.

enriched targets. Consequently, we prioritized in vitro validation of NAF19's regulatory influence on prostate cancer through this pathway. In vitro studies demonstrated that NAF19 markedly suppressed the growth and migratory capacity of LNCaP cells. At the molecular level, mechanistic investigations revealed that NAF19 elevated the E-cadherin expression and simultaneously reduced the levels of Vimentin and N-cadherin. By modulating these key EMT-related markers, NAF19 may reverse the EMT process, contributing to its anti-metastatic potential. Further in vivo findings indicated that NAF19 downregulated key components of the PI3K/Akt signaling axis within prostate tumor specimens. This pathway, a recognized driver of oncogenesis, is often aberrantly activated across multiple cancer types and exerts a critical influence on tumor progression by blocking programmed cell death, overcoming cell cycle checkpoints, and promoting the angiogenesis through the recruitment of vascular endothelial growth factor [24-27].

Our findings confirmed that NAF19 significantly downregulated PI3K, Akt, p-PI3K, and p-Akt. These findings indicate that NAF19 suppresses PCa cell proliferation and differentiation by modulating the PI3K/Akt signaling pathway, which underlies its anti-tumor activity.

Although our study demonstrates that NAF19 suppresses PCa cell growth through inhibition of the PI3K/Akt pathway, KEGG pathway enrichment also highlighted other potentially relevant pathways, such as "Neuroactive ligand–receptor interaction", "Choline metabolism in cancer", and "metabolic reprogramming-related pathways". Whether NAF19 exerts its anti-cancer effects through modulation of these pathways requires further investigation.

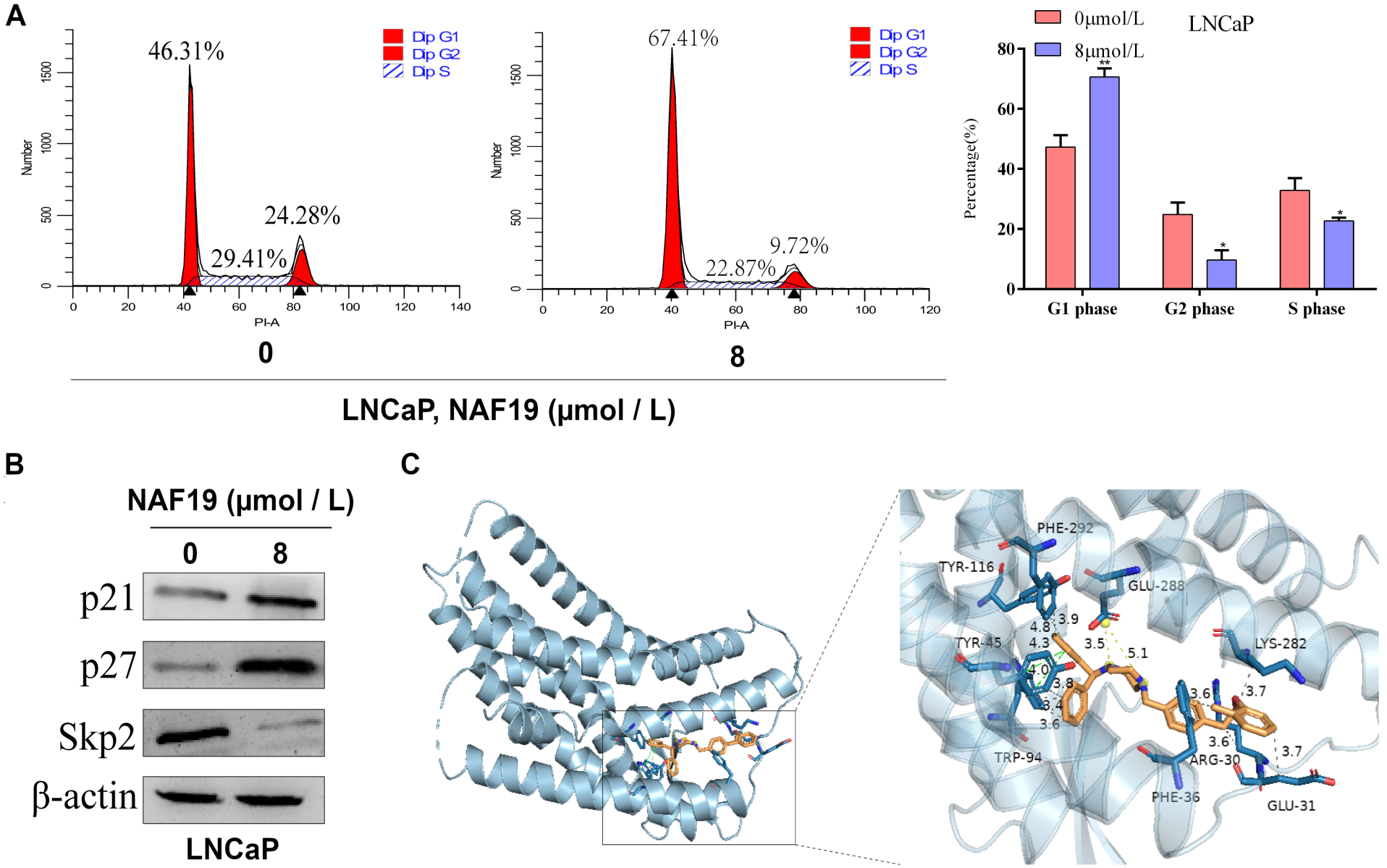

Figure 7. Effect of NAF19 on cell cycle progression in LNCaP cells

(A) Flow cytometry analysis of NAF19-induced cell cycle distribution changes in LNCaP cells; (B) Western blots showing NAF19-mediated alterations in key cell cycle regulatory proteins; (C) Global and local molecular docking diagrams of NAF19 and CXCR4.

The influence of NAF19 on cell cycle progression in PCa cells was further investigated. Treatment with NAF19 led to a pronounced arrest in the G1 phase in LNCaP cells. This effect may be attributed to NAF19's ability to downregulate Skp2 while upregulating P21 and P27. Skp2 plays a crucial role in cell cycle regulation and is closely linked to tumor development and metastatic progression [28-31].

The cell cycle is a fundamental biological process, and its dysregulation is closely linked to cancer development. P21 and P27 are widely recognized as negative regulators of the cell cycle. Skp2 can promote their degradation via the ubiquitin-proteasome pathway [30,32]. Notably, P27 regulates cyclin A and cyclin-dependent kinase 2 (CDK2), leading to G1 phase arrest [33], which aligns with our observation that NAF19 induces G1 phase arrest in LNCaP cells. This suggests that NAF19 may regulate the cell cycle in PCa through the Skp2/P27 signaling axis.

It has been reported that CXCR4 can modulate the expression of Skp2 and its downstream targets by modulation of the PI3K/Akt axis. To explore the possible interaction between NAF19 and CXCR4, molecular docking was performed using AutoDock Vina. This revealed a binding free energy of -9.6 kcal/mol for the NAF19-CXCR4 complex, suggesting a high degree of binding affinity between the compound and the receptor. This supports the hypothesis that CXCR4 may serve as a potential pharmacological target of NAF19. CXCR4 is the most important natural receptor for stromal cell-derived factor-1 (SDF-1). Through a single chemokine–single receptor binding mechanism, it activates downstream signaling pathways and participates in the pathogenesis of malignant tumors [34-36]. Evidence indicates that elevated CXCR4 protein levels are observed during PCa progression, tumor invasion, and metastasis, and are correlated with patient survival outcomes [36,37].

However, whether NAF19 directly targets Skp2 and whether Skp2 regulates P21 and P27 expression through the ubiquitination pathway, remains unclear. Subsequent research will aim to overcome these limitations and provide a more in-depth understanding of the pathways responsible for the anti-tumor activity of NAF19.

CONCLUSIONS

In conclusion, an integrated network pharmacology approach was applied in this research to uncover prospective therapeutic targets of NAF19 against PCa. Additionally, in vitro validation demonstrated that NAF19 markedly suppresses the growth and migratory capacity of PCa cells and promotes G1 cell cycle arrest in LNCaP cells. These effects are potentially mediated through suppression of the PI3K–Akt signaling cascade and modulation of the CXCR4/Skp2/p27 axis.

These results establish a theoretical foundation for developing NAF19 as a promising therapeutic option against PCa, presenting a potential alternative or adjunct to current standard treatments, including androgen deprivation therapy, chemotherapy, and radiation. Furthermore, this study offers new mechanistic insights into NAF19's mode of action, which could aid in the design of more precise and effective targeted therapies for prostate cancer in the future.

ABBREVIATIONS

ANOVA – one-way analysis of variance
AR – androgen receptor
BP – biological process
BPH – benign prostatic hyperplasia
CC – cellular component
CRPC – castration-resistant prostate cancer
DAPI – 4',6-diamidino-2-phenylindole
DMSO – dimethyl sulfoxide
EdU – 5-ethynyl-2′-deoxyuridine
EMT – epithelial-mesenchymal transition
FBS – fetal bovine serum
IC_{50} – half maximal inhibitory concentration
KEGG – Kyoto Encyclopedia of Genes and Genomes
MF – molecular function
NAF19 – naftopidil 19 (novel naftopidil derivative)
PBS – phosphate buffered saline
PCa – prostate cancer
PFA – paraformaldehyde
PPI – protein-protein interaction
SMILES – Simplified Molecular Input Line Entry System

ACKNOWLEDGEMENT

This research was funded by the Scientific and Technological Support Project of Guizhou Province (Grant no. Qian Ke He Zhi Cheng [2023] Yi Ban 262).

AUTHORS' CONTRIBUTION

HJ: conceptualization, validation, formal analysis, writing - original draft preparation, writing - review and editing, funding acquisition.

MX: methodology, formal analysis.

SJ: software, visualization.

WH: investigation, data curation.

HC: resources, writing - original draft preparation.

All authors have read and approved the final version of the manuscript.

CONFLICT OF INTEREST

None to declare.

Publisher's Note: The Editorial Office stays neutral with regard to jurisdictional claims in published maps and institutional affiliations.

REFERENCES

1. Sung H, Ferlay J, Siegel RL, Laversanne M, Soerjomataram I, Jemal A, et al. Global Cancer Statistics 2020: GLOBOCAN Estimates of Incidence and Mortality Worldwide for 36 Cancers in 185 Countries. CA Cancer J Clin. 2024 Oct;18(5):911-920. DOI: 10.3322/caac.21660
2. Siegel RL, Kratzer TB, Giaquinto AN, Sung H, Jemal A. Cancer statistics, 2025. CA Cancer J Clin. 2025 Jan-Feb;75(1):10-45. DOI: 10.3322/caac.21871
3. Zhan H, Zhang S, Li L, Chen Z, Cai Y, Huang J, et al. Naftopidil enantiomers suppress androgen accumulation and induce cell apoptosis via the UDP-glucuronosyltransferase 2B15 in benign prostate hyperplasia. J Steroid Biochem Mol Biol. 2022 Jul;221:106117. DOI: 10.1016/j.jsbmb.2022.106117
4. Ishii K, Matsuoka I, Kajiwara S, Sasaki T, Miki M, Kato M, et al. Additive naftopidil treatment synergizes docetaxel-induced apoptosis in human prostate cancer cells. J Cancer Res Clin Oncol. 2018 Jan;144:89-98. DOI: 10.1007/s00432-017-2536-x
5. Maesaka F, Tanaka N, Nakai Y, Asakawa I, Tomizawa M, Owari T, et al. Comparison of disease-specific quality of life in prostate cancer patients treated with low-dose-rate brachytherapy: A randomized controlled trial of silodosin versus naftopidil. Int J Urol. 2021 Nov;28:1171-1176. DOI: 10.1111/iju.14667
6. Iwamoto Y, Ishii K, Kanda H, Kato M, Miki M, Kajiwara S, et al. Combination treatment with naftopidil increases the efficacy of radiotherapy in PC-3 human prostate cancer cells. J Cancer Res Clin Oncol. 2017 Jun;143(6):933-939. DOI: 10.1007/s00432-017-2367-9
7. Jiang H, Chen H, Wang Y, Xu H, Chen H. Synthesis, bioactivity, and molecular docking studies: novel arylpiperazine derivatives as potential new-resistant AR antagonists. Front Chem. 2025;13:1557275. DOI: 10.3389/fchem.2025.1557275
8. Chen H, Qian Y, Jia H, Yu Y, Zhang H, Shen J, et al. Synthesis and pharmacological evaluation of naftopidil-based arylpiperazine derivatives containing the bromophenol moiety. Pharmacol Rep. 2020 Aug;72(4):1058-1068. DOI: 10.1007/s43440-019-00041-w
9. Zhao Z, Le J, Fu Z, Yang S, Chen Y. Cancer network pharmacology: multi-network regulatory mechanisms and future directions. Med Oncol. 2025 Jun;42(7):255. DOI: 10.1007/s12032-025-02811-4
10. Wang X, Miao YH, Zhao XM, Liu X, Hu YW, Deng DW. Perspectives on organ-on-a-chip technology for natural products evaluation. Food & Medicine Homology. 2025 Sep;145:156985. DOI: 10.26599/FMH.2024.9420013
11. Wang H, Chen T, Wang Y, Li Y, Zhang L, Ding Y, et al. [CXC chemokine receptor 4 regulates breast cancer cell cycle through S phase kinase associated protein 2]. Zhejiang Da Xue Xue Bao Yi Xue Ban. 2017 Jul;46(4):357-363. DOI: 10.3785/j.issn.1008-9292.2017.08.03
12. Quistini A, Chierigo F, Fallara G, Depalma M, Tozzi M, Maggi M, et al. Androgen Receptor Signalling in Prostate Cancer: Mechanisms of Resistance to Endocrine Therapies. Res Rep Urol. 2025;17:211-223. DOI: 10.2147/RRU.S388265
13. Shafi AA, Yen AE, Weigel NL. Androgen receptors in hormone-dependent and castration-resistant prostate cancer. Pharmacol Ther. 2013 Dec;140(3):223-38. DOI: 10.1016/j.pharmthera.2013.07.003
14. Abd Wahab NA, Lajis NH, Abas F, Othman I, Naidu R. Mechanism of Anti-Cancer Activity of Curcumin on Androgen-Dependent and Androgen-Independent Prostate Cancer. Nutrients. 2020 Mar;12(3). DOI: 10.3390/nu12030679
15. Fang F, Qin Y, Hao F, Li Q, Zhang W, Zhao C, et al. CD147 modulates androgen receptor activity through the Akt/Gsk-3β/β-catenin/AR pathway in prostate cancer cells. Oncol Lett. 2016 Aug;12(2):1124-1128. DOI: 10.3892/ol.2016.4684
16. Crisafi D, Wong BNX, Bolton D, Ischia J, Woon D. Urologist underutilisation of androgen receptor pathway inhibitors for metastatic hormone-sensitive prostate cancer. BJU Int. 2024 Dec;(0):12-13. DOI: 10.1111/bju.16570
17. Cole RN, Fang Q, Matsuoka K, Wang Z. Androgen receptor inhibitors in treating prostate cancer. Asian J Androl. 2025 Mar;27(2):144-155. DOI: 10.4103/aja202494
18. Pisano C, Tucci M, Di Stefano RF, Turco F, Scagliotti GV, Di Maio M, et al. Interactions between androgen receptor signaling and other molecular pathways in prostate cancer progression: Current and future clinical implications. Crit Rev Oncol Hematol. 2021 Jan;157:103185. DOI: 10.1016/j.critrevonc.2020.103185
19. Pearson HB, Li J, Meniel VS, Fennell CM, Waring P, Montgomery KG, et al. Identification of Pik3ca Mutation as a Genetic Driver of Prostate Cancer That Cooperates with Pten Loss to Accelerate Progression and Castration-Resistant Growth. Cancer Discov. 2018 Jun;8(6):764-779. DOI: 10.1158/2159-8290.CD-17-0867
20. Guo R, Shi L, Chen Y, Lin C, Yin W. Exploring the roles of ncRNAs in prostate cancer via the PI3K/AKT/mTOR signaling pathway. Front Immunol. 2022 May;80:1-17. DOI: 10.3389/fimmu.2025.1525741
21. Tewari D, Patni P, Bishayee A, Sah AN, Bishayee A. Natural products targeting the PI3K-Akt-mTOR signaling pathway in cancer: A novel therapeutic strategy. Semin Cancer Biol. 2022 May;80:1-17. DOI: 10.1016/j.semcancer.2019.12.008
22. Sarker D, Reid AH, Yap TA, de Bono JS. Targeting the PI3K/AKT pathway for the treatment of prostate cancer. Clin Cancer Res. 2009 Aug 1;15(15):4799-805. DOI: 10.1158/1078-0432.CCR-08-0125
23. Marques RB, Aghai A, de Ridder CMA, Stuurman D, Hoeben S, Boer A, et al. High Efficacy of Combination Therapy Using PI3K/AKT Inhibitors with Androgen Deprivation in Prostate Cancer Preclinical Models. Eur Urol. 2015 Jun;67(6):1177-1185. DOI: 10.1016/j.eururo.2014.08.053
24. Hoxhaj G, Manning BD. The PI3K-AKT network at the interface of oncogenic signalling and cancer metabolism. Nat Rev Cancer. 2020 Feb;20(2):74-88. DOI: 10.1038/s41568-019-0216-7
25. Araki K, Miyoshi Y. Mechanism of resistance to endocrine therapy in breast cancer: the important role of PI3K/Akt/mTOR in estrogen receptor-positive, HER2-negative breast cancer. Breast Cancer. 2018 Jul;25(4):392-401. DOI: 10.1007/s12282-017-0812-x

26. Noorolyai S, Shajari N, Baghbani E, Sadreddini S, Baradaran B. The relation between PI3K/AKT signalling pathway and cancer. Gene. 2019 May;698:120-128. DOI: 10.1016/j.gene.2019.02.076

27. He Y, Sun MM, Zhang GG, Yang J, Chen KS, Xu WW, et al. Targeting PI3K/Akt signal transduction for cancer therapy. Signal Transduct Target Ther. 2021 Dec;6(1):425. DOI: 10.1038/s41392-021-00828-5

28. Peng Y, Qi X, Ding L, Huang J, Liu Y, Zheng R, et al. SKP2 inhibition activates tumor cell-intrinsic immunity by inducing DNA replication stress and genomic instability. Br J Cancer. 2025 Jan;132(1):81-92. DOI: 10.1038/s41416-024-02909-y

29. Brown LK, Kanagasabai T, Li G, Celada SI, Rumph JT, Adunyah SE, et al. Co-targeting SKP2 and KDM5B inhibits prostate cancer progression by abrogating AKT signaling with induction of senescence and apoptosis. Prostate. 2024 Jun;84(9):877-887.. DOI: 10.1002/pros.24706

30. Feng T, Wang P, Zhang X. Skp2: A critical molecule for ubiquitination and its role in cancer. Life Sci. 2024 Feb; 1:338:122409. DOI: 10.1016/j.lfs.2023.122409

31. Rezaeian AH, Phan LM, Zhou X, Wei W, Inuzuka H. Pharmacological inhibition of the SKP2/p300 signaling axis restricts castration-resistant prostate cancer. Neoplasia. 2023 Apr;38:100890. DOI: 10.1016/j.neo.2023.100890

32. Asmamaw MD, Liu Y, Zheng YC, Shi XJ, Liu HM. Skp2 in the ubiquitin-proteasome system: A comprehensive review. Med Res Rev. 2020 Sep;40(5):1920-1949. DOI: 10.1002/med.21675

33. Liu J, Peng Y, Shi L, Wan L, Inuzuka H, Long J, et al. Skp2 dictates cell cycle-dependent metabolic oscillation between glycolysis and TCA cycle. Cell Res. 2021 Jan;31(1):80-93. DOI: 10.1038/s41422-020-0372-z

34. Park C, Lee JW, Kim K, Seen DS, Jeong JY, Huh WK. Simultaneous activation of CXC chemokine receptor 4 and histamine receptor H1 enhances calcium signaling and cancer cell migration. Sci Rep. 2023 Feb;13(1):1894. DOI: 10.1038/s41598-023-28531-1

35. D'Agostino G, Cecchinato V, Uguccioni M. Chemokine Heterocomplexes and Cancer: A Novel Chapter to Be Written in Tumor Immunity. Front Immunol. 2018;9:2185. DOI: 10.3389/fimmu.2018.02185

36. Gupta N, Ochiai H, Hoshino Y, Klein S, Zustin J, Ramjiawan RR, et al. Inhibition of CXCR4 Enhances the Efficacy of Radiotherapy in Metastatic Prostate Cancer Models. Cancers (Basel). 2023 Feb 6;15(4). DOI: 10.3390/cancers15041021

37. Zhu WB, Zhao ZF, Zhou X. AMD3100 inhibits epithelial-mesenchymal transition, cell invasion, and metastasis in the liver and the lung through blocking the SDF-1α/CXCR4 signaling pathway in prostate cancer. J Cell Physiol. 2019 Jul;234(7):11746-11759. DOI: 10.1002/jcp.27831